Mater. Res. Soc. Symp. Proc. Vol. 1207 © 2010 Materials Research Society 1207-N03-08

Post-Synthesis Crystallinity Tailoring of Water-Soluble Polymer Encapsulated CdTe Nanoparticles using Rapid Thermal Annealing

Steven Rutledge[1], Abdiaziz A. Farah[1], Jordan Dinglasan[2], Darren Anderson[2], Anjan Das[2], Jane Goh[3], Cynthia Goh[3], and Amr S. Helmy[1*]

[1]The Edward S. Rogers Sr. Department of Electrical and Computer Engineering, University of Toronto, 10 Kings College, Toronto, Ontario M5S 3G4 (Canada), [2] Vive Nano Incorporated, 80 St. George St, Toronto, Ontario M5S 3H6 (Canada), [3] Department of Chemistry, University of Toronto, 80 St. George St, Toronto, Ontario M5S 3H6 (Canada)

ABSTRACT

The crystallinity of colloidal CdTe nanoparticles has been enhanced post synthesis. This control over the nanoparticles' properties has been achieved using non-adiabatic thermal processing. The technique preserves the polymer capping and hence introduces no adverse effects on the nanoparticles' optical properties. The crystallinity is probed primarily through Raman spectroscopy in a hollow core photonic crystal fiber and x-ray diffraction powder studies.

INTRODUCTION

The process of rapid thermal annealing (RTA) has been applied extensively in semiconductor processing and has been demonstrated to provide numerous benefits in semiconductor systems [1]. RTA has been used to influence the photoluminescence (PL) efficiency, size dispersion and compositional intermixing for epitaxial grown or implanted quantum dots (QDs) [1,2]. However, its influence on the properties of polymer capped nanostructures has not yet been investigated. If characterized, the influence of RTA on colloidal nanostructures can present an attractive processing technique. It can be a particularly enabling processing technology as shown in the case of PEDOT-PSS thin films to influence morphological and microstructural change of this semiconducting polymer while preserving its molecular integrity [3]. NPs of numerous shapes, sizes, and compositions have been reported over the past two decades and continue to exhibit exciting optical and electrical characteristics [4]. In particular, II-VI semiconductor CdTe NPs have been demonstrated suitable for use in applications involving efficient solar cells, ultrafast electron transfer, and negative refractive index materials [5-7]. This study reports on the ability to influence the degree of crystallinity of polymer stabilized CdTe NPs using RTA. Raman spectroscopy, PL, UV-visible absorption, X-ray photoelectron spectroscopy (XPS), and X-ray diffraction (XRD), have been utilized to analyze the crystalline changes in the polymer capped CdTe NPs.

DISCUSSION

Dried carboxylate functionalized CdTe NPs obtained from *Vive Nano* are annealed in inert Argon gas conditions for 30 seconds before a cool off period. The annealing temperature ranges from 200ºC to 600ºC in 100ºC increments with the ramping temperature maintained at a constant 50ºC/s gradient in all cases. All annealing is performed in an *AnnealSys AS-One* rapid thermal annealing system. The sample is then reweighed and dispersed in water to achieve NP concentrations of 2 mg/mL.

The most exciting characteristic of the annealing process was initially identified using a hollow-core photonic crystal fiber (HC-PCF) based Raman scan. Raman scans were performed using a *Horiba Jobin Yvon H800* integrated Raman system along with the HC-PCF waveguiding technique developed by Irizar et al. [8]. With the enhanced sensitivity of this method, three Raman active peaks in the dispersed solution could be identified as shown in **(Fig. 1)**.

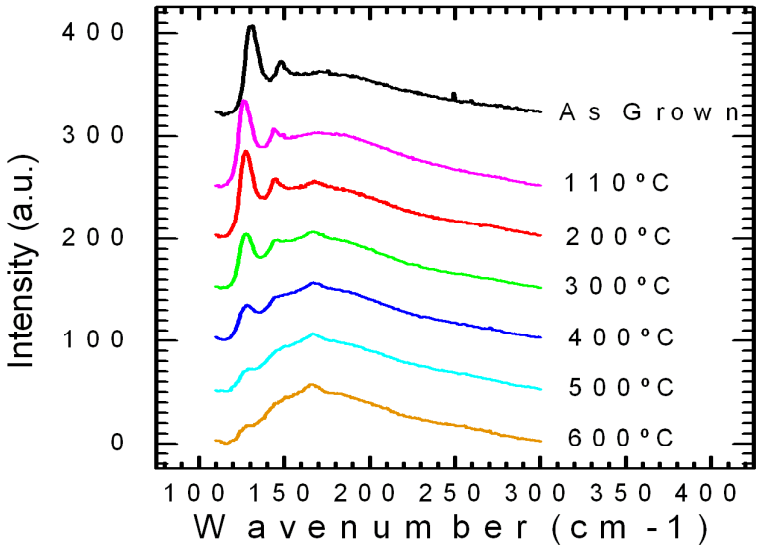

Figure 1. Raman spectra of annealed and as-grown NPs up to 600ºC

These three peaks correspond to the Te A1 mode at ~127 cm^{-1}, the Te E mode at ~141 cm^{-1}, and the CdTe LO mode at ~165 cm^{-1} [9-11]. Due to the modes' finite width and hence overlapping frequencies, there could also be a portion of the Te E peak contributed by the CdTe TO phonon mode which is located at ~140 cm^{-1}. The presence of the two Te peaks have been attributed to Te inclusions within the center of the crystal or surface defects along the boundaries of the material [9-11]. It is difficult to quantify from the Raman measurements the amount of Te inclusions or defects, due to the fact that Te crystals exhibit a relatively high Raman scattering signal in comparison to CdTe as a result of unequal Raman cross-sections [10,12]. Following a baseline correction and peakfitting routine, Gaussian-Laurentzian peaks were fitted to the Raman spectra for analysis. **(Fig. 2)** shows a reduction in the intensity ratios of the Te phonon peaks in relation to the CdTe modes. When comparing the Te A1 mode to the CdTe LO mode, an intensity ratio of 19.52 is obtained in the 200ºC annealed sample, which decreases to a minimum of 2.20 in the 600ºC annealed sample. Similarily, the ratio between the Te E peak and the CdTe LO peak decreases in the same manner from 10.47 to 0.65. This intensity decrease of the Raman active Te modes indicates the reduction in Te inclusions or surface defects within the NP and capping structure. Two additional samples were investigated: the NPs being annealed at the minimum temperature possible (110ºC), and of the NPs undergoing the atmospheric processing routine (vacuum followed by Argon) but with no heat applied. Neither of these samples displayed any obvious differences from the Raman spectra of the unannealed NPs.

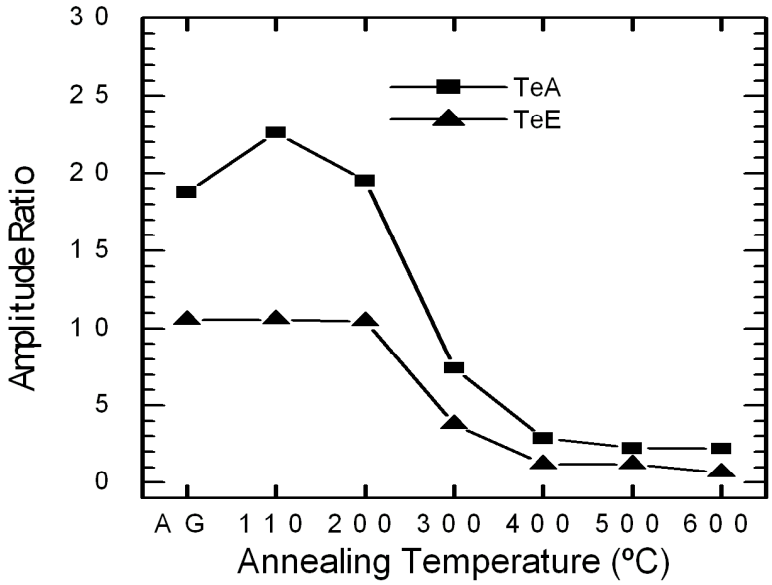

Figure 2. Raman Te A1 and E modes vs. CdTe LO mode amplitude ratio.

What can be seen from the Raman scans is the progressive decrease in amplitude ratios between the Te and CdTe modes with increase of annealing temperature. While there is little change in the 200ºC annealed sample, the ratios drop by around 50% in the 300ºC and even further in the higher temperature anneals. It is significant to note that the majority of the transition occurs with annealing temperatures between 200ºC and 400ºC, with little change between as-grown and the 200ºC annealed sample nor with annealing temperatures above 400ºC. This leads to the conclusion that the annealing is affecting the NPs by reducing the Te inclusions or surface defects from the semiconductor core most dramatically between the temperatures of 200ºC and 400ºC. Increasing temperature while maintaining the constant anneal times, progressively moves the samples further along in a crystallization mechanism and thus the aformentioned Raman peak ratios are obtained.

A room temperature PL was performed using a *Tecan Safire* system. The results shown in **(Fig. 3A)** indicate that there is a notable reduction in PL intensity starting with samples annealed above 400ºC. This is in high contrast to the effects of traditional annealing of semiconductor NPs in a polymer matrix, where significant PL reduction was observed at lower temperature (140ºC and 180ºC) anneals [13]. The fact that PL stays approximately constant at high temperatures in the RTA mechanism offers increased processing options in manufacturing and research. The observed reduction in PL intensity is attributed to an increase in the density of trapped states on the surface of the NPs, where non radiative processes are dominant. This density increase arises due to changes in interactions between the organic protecting layer and the CdTe NP surface. It is noteworthy to mention that the position and the shape of PL profiles were unchanged albeit with a slight red shift of approximately 5 nm in the 600ºC annealed sample. This indicates that the annealing does not significantly affect the size of CdTe NPs, since the PL wavelength is subject to the quantum size effect and thus directly dependent on particle size.

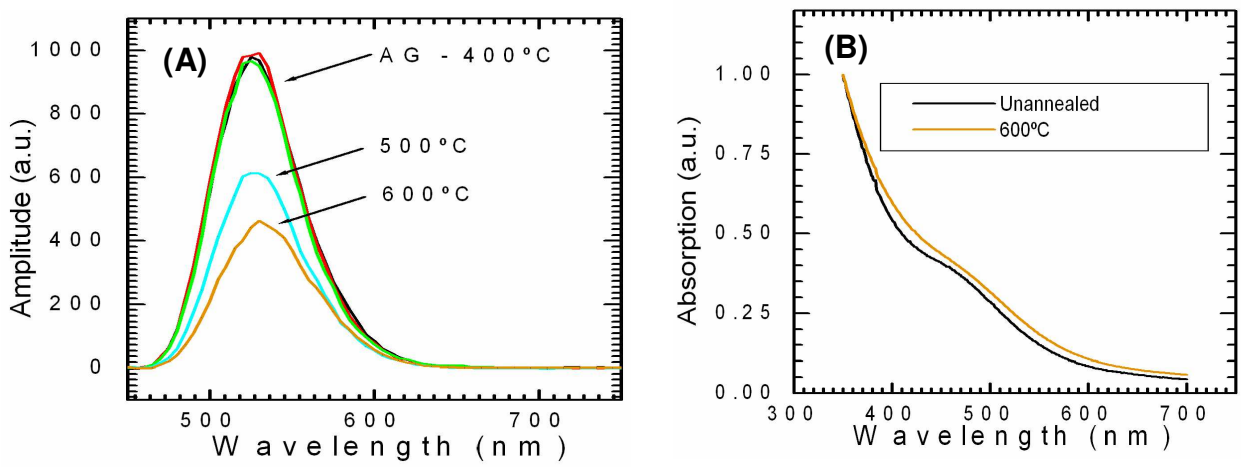

Figure 3. (A) PL spectra of annealed and as-grown NPs. The spectra of the as-grown, 200ºC, 300ºC, and 400ºC annealed samples are overlapping and have thus been labelled together. (B) UV-vis absorption spectra of as-grown and 600ºC annealed sample.

The use of the a UV-absorption scan shown in **(Fig. 3B)** corroborates the PL conclusion that the size of the NPs are unchanged since the absorption spectra remains unvaried except for the slight red shift of the absorption shoulder in the 600ºC annealed sample. Due to the fact that the NPs are maintaining a constant size also means that the polymer capping layer is still present in some form even at 600ºC annealing temperature. While there are some changes in the polymer attributing to the loss in PL intensity in the high temperature anneals, the quantum confinement of these NPs are preserved in all samples. Utilizing an RTA process allows for much higher temperature anneals in comparison to traditional annealing processes, without affecting the PL and maintaining an intact polymer capped NP.

An insight into the structural features of these polymer stabilized NPs was obtained from the transmission electron microscopy (TEM) pictures. TEM reveals CdTe NPs of nominally constant size as is evident in **(Fig 4a)** taken from the unannealed sample. The NPs have a diameter on the order of 4-5nm. Critical to any potential application of these CdTe NPs is their thermal and optical stability after exposure to thermal treatment. Notably, as can be seen in **(Fig. 4b)**, the CdTe NPs did not grow in size during the RTA process at 600ºC. TEM was taken on all other temperature samples and the size of the NPs remained constant. This finding is in contrast to an earlier finding by Mehta et.al, wherein furnace annealed CdTe NPs dispersed in SiO2 film grew in size [14]. Similarily, in another study, the size of aqueous grown CdTe NPs was also seen to increase with higher annealing temperatures according to Bandaranyake et. al, in a conventional annealing environment [15]. The fact that under the RTA process these CdTe NPs retain their initial size is significant for future QD implementation into opto-electronic devices. This invariance of NP size as seen from TEM, corroborates with the PL and UV-absorption results.

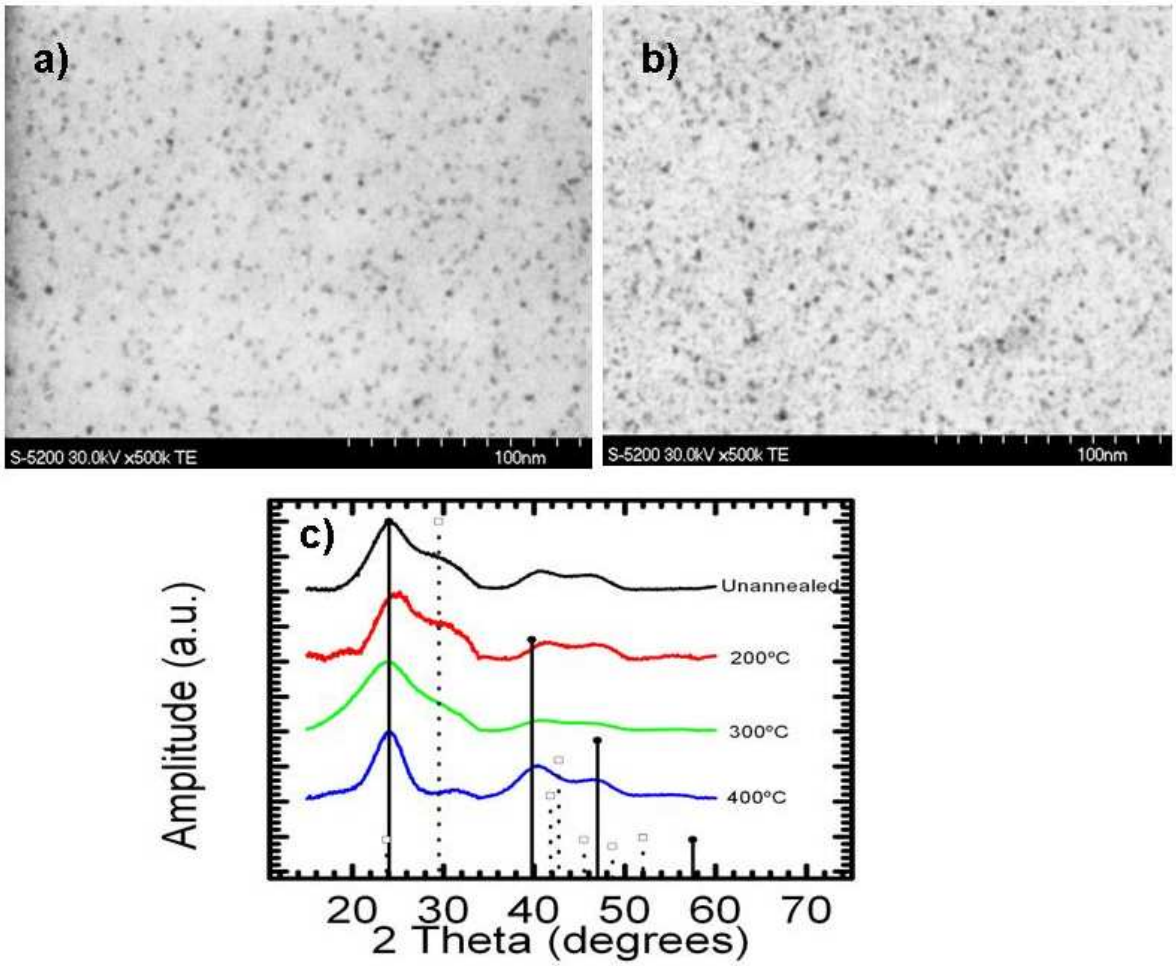

Figure 4. TEM image of (a) as-grown sample and (b) 600ºC annealed sample. (c) an overelay spectra of XRD of as-grown samples and 200, 300 and 400ºC annealed samples. Powder diffraction lines of wurzite (□) and zincblende (*) type crystalline CdTe markers are also shown as references.

XRD measurements allow for identification of crystalline phases in the NPs, however it is not as sensitive as the Raman technique to the relatively small changes that are occuring [10]. In **(Fig. 4c)**, the XRD results are shown along with the significant powder diffraction lines characteristic of wurzite and zincblende CdTe (pictured on the bottom of **(Fig. 4c)** as square outlines and solid circles respectively). The XRD results display broad features with no sharp crystalline peaks in contrast to what would be expected in highly crystalline materials. There are three highly identifiable peaks located at approximately 24º, 40º, and 46º that indicate the presence of a zincblende structure and corrolate to reflections from the 111, 220, and 311 planes respectively. However, another feature present most clearly in the unannealed and 200ºC annealed samples is a shoulder off of the 111 peak at around the 29º mark. This feature may be attributed to irregularities and randomizations present in the crystal characteristic of the growth procedure or it could corrolate to the 102 plane found in a wurzite CdTe structure. This conclusion corroborates with previously documented research into the annealing of CdTe Qds

where the zincblende form of CdTe prevailed regardless of temperature [15]. While there is a slight increase of the FWHM of the zinblende 111 crystalline peak in the 300ºC annealed sample, the feature at 29º has already been substantially reduced indicating a prevalence in the zincblende structure. In the 400ºC annealed sample, the core has crystallized into a clear zincblende structure identified by a decrease in FWHM of the 111 peak, combined with the disappearance of the extraneous 29º feature. This crystalline reorganization occurs over the same temperature range in which the Raman mode ratios were seen to vary the greatest. The crystalline change being observed can be attributed to one of two things. In the first reasoning, if it is assumed that the feature at 29º is a result of the 102 plane in wurzite CdTe, the RTA process above 200ºC acts to remove the wurzite form CdTe within the NP, and thus reducing grain boundaries. This in turn will both account for the trends seen in the XRD measurements but also the Raman mode ratio trends, since with less grain boundaries, the amount of surface defects between crystal phases and subsequent Te-Te bonds will be decreased. On the other hand, if the feature at 29º is attributed to randomizations in the crystal due to the growth mechanisms, the RTA process operates to remove these crystal defects and randomizations, as demonstrated through both the XRD spectra and also the Raman mode ratio trends. Regardless, what is significant is that the fact the the semiconductor core after the RTA process is displaying an enhanced level of crystallinity that is not present in the as-grown NP. This enhancement in the core, can be vital to potential QD devices that rely on a high degree of core crystallinity and the ability to increase the crystal core using current processing techniques is of extreme value.

CONCLUSIONS

In conclusion, this study attests that through RTA process, the semiconductor core of CdTe NPs can be influenced to develop a higher degree of crystallinity as compared to the unprocessed materials. This crystalline shift has been verified by both Raman spectroscopy in a HC-PCF liquid core waveguide, and an XRD scans. Combined with the tailoring of the crystalline core, the size of the NPs remains stable with temperature, in contrast with the growth in size observed with NPs that have undergone a traditional annealing process.
Although much research is still needed to optimize polymer encapsulated QD materials fabrication and processing, to the best of our knowledge this is a first step towards the integration of polymer capped inorganic NPs into current semiconductor manufacturing techniques, where such QDs have shown to possess great potential.

ACKNOWLEDGMENTS

Ontario Centre for Excellence (OCE)(Research Fund 72032825) is acknowledged for financial support. We are also grateful to Battista Calvieri and the microscopy imaging laboratory, Faculty of Medicine (U of T) for TEM images

REFERENCES

[1] R. Singh, *J. Appl. Phys.* **63**, R59. (1998),
[2] D. Bhattacharayya, A. S. Helmy, A. C. Bryce, E. A. Avrutin, J.H. Marsh, *J. Appl. Phys.* **88**, 4619 (2000)
[3] A. Schaarschmidt, A. A. Farah, A. Aby, A. S. Helmy, *J. Phys. Chem.* B **113**, 9352 (2009)

[4] a) C. B. Murray, C. R. Kagan, M. G. Bawendi. *Annu. Rev. Mater. Sci.*, **30**, 545 (2000). b) M. G. Bawendi, M. L. Steigerwald, L. E. Brus. *Annu. Rev. Phys. Chem.*, **41**, 477 (1990). c) A. P. Alivisatos. *Science* **271**, 933 (1996). d) R. C. Somers, M. G. Bawendi, D. C. Nocera, *Chem. Soc. Rev*., **36**, 579 (2007).

[5] Y. Kang, N. Park, D. Kim. *Appl. Phys. Lett.*, **86**, 113101 (2005).

[6] C. Dooley, S. Dimitrov, T. Fiebig, *J. Phys. Chem. C,* **112**, 12074 (2008).

[7] A. Agarwal, G. Lilly, A. Govorov, N. Kotov, *J. Phys. Chem. C,* **112**, 18314 (2008).

[8] J. Irizar, J. Dinglasan, J. B. Goh, A. Khetani, H. Anis, D. Anderson, C. Goh, A. S. Helmy, *IEEE J. Select. Top. Quant. Electron.*, **14**, 1214 (2008).

[9] O. Ochoa, E. Witkowski III, c. Colajacomo, J. Simmons, B. Potter Jr, *J. Mat. Sci. Lett.,* **16***,* 613 (1997)

[10] G. Morell, A. Reynés-Figueroa, R. Katiyar, M. Farias, F. Espinoza-Beltran, O. Zelaya-Angel, F. Sánchez-Zinencio, *J. Raman Spectroscopy*, **25**, 203 (1994).

[11] V. Vinogradov, G. Karczwski, I. Kucherenko, N. Mel'nik, P. Fernadez, *Physics of the Solid State*, **50**, 164 (**2008)**.

[12] F. Caballero-Briones, A. Zapata-Navarro, A. Martel, A. Iribarren, J. Peña, R. Castro-Rodríguez, P. Bartolo-Pérez, F. Rábago-Bernal, S. Jiménez-Sandoval, *Superfices y Vacio*, **16**, 38 (2003).

[13] Y. –H. Niu, A. M. Munro, Y. –J. Cheng, Y. Tian, M. S. Liu, J. Zhao, J. A. Bardecker, I. J. –L. Plante, D. S. Ginger, A. K. –Y. Jen, *Advanced Materials*, **19**, 3371 (2007).

[14] P. B. Dayal, B. R. Mehta, S. M. Shivaprasad, *Jpn. J. Appl. Phys*., **44**, 8222 (2005).

[15] R. J. Bandaranayake, G. W. Wen, J. Y. Lin, H. X. Jiang, C. M. Sorenson, *Appl. Phys. Lett,* **6**, 831 (1995).